Shock-produced akimotoite in the Suizhou L6 chondrite

CHEN Ming[1,2] & XIE XianDe[2*]

[1] *State Key Laboratory of Isotope Geochemistry, Guangzhou Institute of Geochemistry, Chinese Academy of Sciences, Guangzhou 510640, China;*
[2] *Key Laboratory of Mineralogy and Metallogeny, Guangzhou Institute of Geochemistry, Chinese Academy of Sciences, Guangzhou 510640, China*

Shock-produced akimotoite was identified in the Suizhou chondritic meteorite, which occurs in two kinds of occurrence. The first is the irregular layers of akimotoite up to 4 µm in thickness occurring in fractures and cracks of low-Ca pyroxene enclosed in the shock veins. The second is the zonal polycrystalline aggregates of akimotoite in shocked pyroxene grains close to the shock vein, where akimotoite occurs in a zonal area in between pyroxene and $MgSiO_3$-glass as irregular small clumps up to 5 µm in size. This investigation suggests a solid-state transformation mechanism of pyroxene to akimotoite, and that akimotoite should have nucleated and grew in the area with abundant defects caused by shock deformation because the defect significantly enhances the solid-state reactivity and the kinetics of nucleation of high-pressure phase. The spatial relationship among the composed grains of pyroxene, akimotoite and $MgSiO_3$-glass (possibly vitrified perovskite) demonstrates a temperature gradient from the vein wall to the unmelted chondritic meteorite.

At high pressure and temperature, (Mg, Fe) SiO_3 pyroxene transforms to high-pressure polymorphs including majorite, akimotoite and perovskite. These high-pressure polymorphs of pyroxene are potentially important mantle minerals that have not been previously found in terrestrial rocks. However, they have been identified in the shock melt veins of chondritic meteorites. Majorite has been found in more than 12 ordinary L- and H-group chondrites, but akimotoite and vitrified perovskite were found only in several L-group chondrites (Xie et al., 2011).

Sharp et al. (1997) found $MgSiO_3$-ilmenite (i.e. akimotoite) and amorphous $MgSiO_3$ glass in the shock veins of the Acfer 040 (L5-6) chondrite, and the later was considered to be the material of vitrified $MgSiO_3$-perovskite after pressure release. Both high-pressure polymorphs were explained to have crystallized from shock-produced silicate melt at high pressures. At the same time, Tomioka et al. (1997) also independently discovered the $MgSiO_3$-ilmenite and possibly the $MgSiO_3$-perovskite inside the shock veins in the Tenham L6 chondrite: This $MgSiO_3$-ilmenite was than approved as a new mineral with the mineral name akimotoite (Tomioka and Fujino, 1999). Both phases were inferred to have transformed from pyroxene at high pressures and temperatures via solid-state mechanisms. Since then, akimotoite has been identified in some other shock-metamorphosed meteorites, such as Umbarge (Xie and Sharp, 2004), Suizhou (Xie et al., 2005), Yamato 791384 (Ohtani et al., 2004), Sixiangkou (Zhang, 2006), and NWA-5011 (Nagy et al., 2010).

Ferroir et al. (2008) reported observations of four textural relationships between pyroxene and akimotoite in the Ten-

ham L6 chondrite. They suggested that shock-produced akimotoite is mainly formed by solid-state transformation of former pyroxenes with subsequent diffusion of calcium, aluminum and sodium from the chondritic melt of the shear melt vein.

Suizhou L6 chondrite is a shocked meteorite with occurrence of thin shock melt veins less than three hundred micrometers in thickness. The shock veins contains abundant high-pressure polymorphs including ringwoodite, majorite, majorite-pyrope garnet, akimotoite, magnesiowüstite, lingunite, tuite, xieite (Xie et al., 2001, 2003, 2005, 2011; Chen et al., 2003a, 2003b, 2004, 2008). A (Mg, Fe) SiO_3-glass was also identified in the shock veins, which was suggested to be possibly a vitrified perovskite (Chen et al., 2004). In this paper, we report a unique occurrence of akimotoite in the meteorite different from previous reports, which could have implication for its formation mechanism.

1   Samples and methods

The Suizhou meteorite is an L6 (S5) chondrite and is consisted of olivine, low-Ca pyroxene, plagioclase, FeNi metal, troilite, whitlockite, chlorapatite, chromite and ilmenite (Xie et al., 2001, 2003). Most plagioclase grains in the meteorite were shock-melted and transformed to maskelynite. This meteorite contains very thin shock-produced melt veins ranging from 20 to 220 μm in width (Figure 1). These shock veins are chondritic in composition and contain abundant high-pressure minerals. The shock-produced pressure and temperature were estimated to be up to 22 GPa and 1000°C for the Suizhou unmelted chondritic rock, and 23 GPa and 2000°C for the shock veins (Xie et al., 2001, 2003).

Polished thin sections of the Suizhou meteorite were prepared from the vein-bearing fragments. The petrology and compositions of minerals were investigated by an optical microscope and a Hitachi S-3500N scanning electron
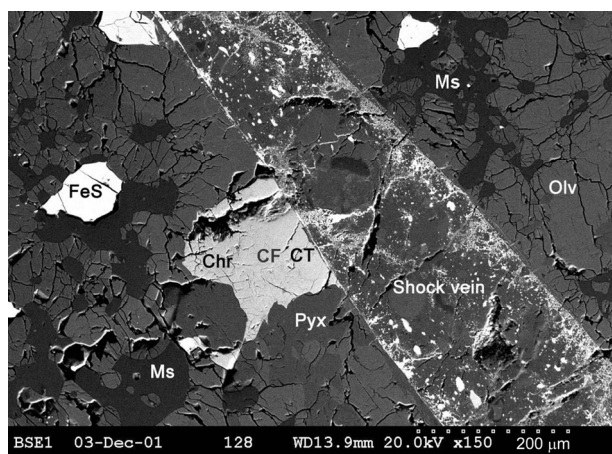
microscope (SEM) in back-scattered electron (BSE) mode that is equipped with a Link ISIS 300 energy dispersive spectrometer (EDS). Chemical composition of low-Ca pyroxene was also analyzed by a JEOL JXA-8100 electron microprobe (EMP) at 15 kV accelerating voltage and 10 nA beam current. Raman spectra of minerals were recorded with a Renishaw R-2000 instrument. A microscope was used to focus the excitation beam (Ar+ laser, 514 nm line) to 2 μm wide spots and to collect the Raman signal. Accumulations of the signal lasted 120 to 150 s. The laser power was 26.8 mW.

2   Results

2.1   Occurrence

The first occurrence of akimotoite in the Suizhou meteorite displays as irregular layers up to 4 μm in thickness within low-Ca pyroxene enclosed in shock veins. Figure 2 shows an ovoid fragment of chondritic meteorite consisting of pyroxene and olivine that is enclosed in the shock vein, and akimotoite occurs as thin layers. On the BSE image, akimotoite shows grey color which is a bit lighter than the dark low-Ca pyroxene. The boundaries of akimotoite-layers are not sharp, and show jagged surface. It indicates that the akimotoite is polycrystalline aggregates grown along fractures and cracks in pyroxene. The single crystal of akimotoite is too small to observe its crystal form under this magnification of BSE image.

The second occurrence is the zonal polycrystalline aggregates of akimotoite in shocked pyroxene grains close to the shock vein, where akimotoite occurs as irregular small clumps up to 5 μm in size. The single crystal form of akimotoite could not be observed under this magnification of BSE image. Figure 3 shows an akimotoite-bearing low-Ca pyroxene grain close to shock vein. One side of the pyroxene in contact with shock vein was transformed to
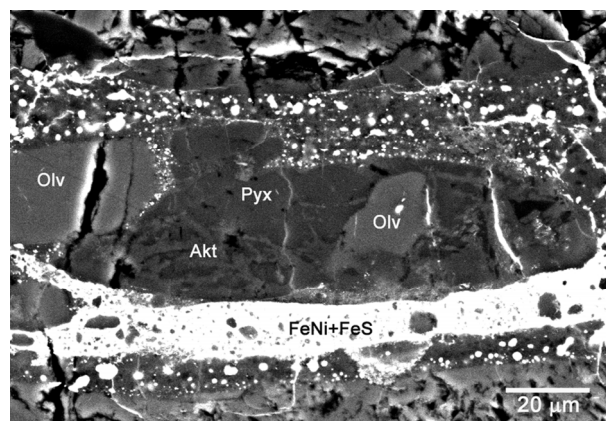

Figure 1   BSE image showing a shock vein in the Suizhou meteorite. CT=xieite, CF=calcium ferrite-structured $FeCr_2O_4$, Chr=chormite, Olv= olivine, Pyx=pyroxene, Ms=maskelynite, FeS=troilite.

Figure 2   BSE image of an ovoid fragment of chondritic rock in the Suizhou shock vein. Note the occurrence of akimotoite (Akm) along fractures and cracks inside a low-Ca pyroxene (Pyx) fragment. Olv=olivine, FeNi+FeS=metal+troilite intergrowth.
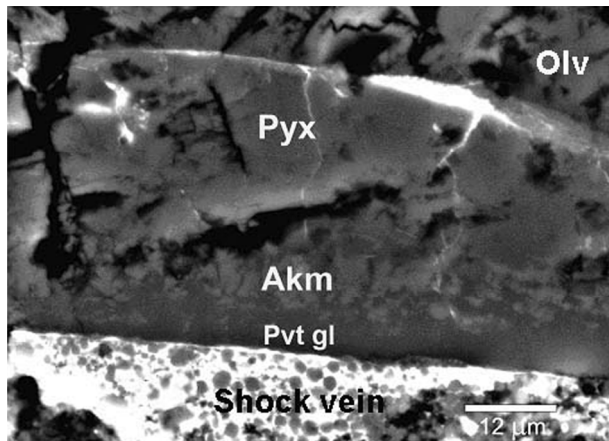
Figure 3　BSE image showing zonal akimotoite (Akm) in between pyroxene (Pyx) and (Mg, Fe)SiO₃-glass (Pvt gl). The (Mg, Fe) SiO₃-glass is in direct contact with shock vein. Olv=olivine.

MgSiO₃-glass up to 10 μm in width. Akimotoite occurs in a zonal area between pyroxene and MgSiO₃-glass. The MgSiO₃-glass also occurs in a narrow zone with width about 10 μm in contact with the shock veins. The distance from the region of akimotoite to the wall of shock vein is from 5 to 10 μm.

2.2　Chemical compositions

Results of electron microprobe analyses show that low-Ca pyroxene has the composition with chemical formula of $(Mg_{0.78}Fe_{0.21}Ca_{0.02})_{1.01}(Si_{0.98}Al_{0.01})_{0.99}O_3$ (Table 1). The compositions of akimotoite and (Mg, Fe)SiO₃-glass were analyzed by energy dispersive spectroscopy (EDS) because the area of akimotoite is too small to be analyzed by electron microprobe. The composition of low-Ca pyroxene was also analyzed by EDS for a comparison of analyses between EDS and EPMA. It shows that analytical result of EDS is similar to that of EPMA. Our analyses show that akimotoite

Table 1　Chemical compositions of low-Ca pyroxene, akimotoite, and (MgFe)SiO₃-glass (wt%)[a]

Oxides	Low-Ca pyroxene*	Low-Ca pyroxene	Akimotoite	(MgFe)SiO₃-glass
FeO	13.70	13.76	13.71	13.88
MgO	27.94	27.86	27.79	27.65
MnO	0.44	0.47	0.45	0.44
CaO	0.78	0.86	0.89	0.90
K₂O	0.01	0.03	0.05	0.04
Na₂O	0.03	n.d.	n.d.	0.05
Al₂O₃	0.19	0.21	0.24	0.30
Cr₂O₃	0.13	0.18	0.16	0.16
TiO₂	0.20	0.19	0.16	0.17
SiO₂	56.38	56.44	56.55	56.41
Total	99.80	100	100	100

a) * means average of 4, analyzed by EPMA, all other data are measured by EDS. n.d. means not detected.

has an identical composition as low-Ca pyroxene and (Mg, Fe)SiO₃-glass (Table 1), although the brightness of akimotoite is higher than the latter two on the BSE images due to their changes in densities or structures.

2.3　Raman spectroscopy

Raman spectrum of the Suizhou low-Ca pyroxene shows bands at 1014, 927, 793, 677, 658, 520, 407, 385, 335 and 233 cm⁻¹ (Figure 4(a)). Raman spectrum of akimotoite displays bands at 798, 678, 614, 478, 406 and 344 cm⁻¹ with typical strong peak at 798 cm⁻¹ corresponding to the stretching vibrations of the SiO₄ tetrahedra (Figure 4(b)), which is in good agreement with the Raman spectra of akimotoites identified in other L-group chondrites (Ohtani et al., 2004; Zhang, 2006; Nagy et al., 2010; Ferroir et al., 2008). Raman bands of akimotoite in the Suizhou meteorite are much sharper than those in other chondrites, hence indicating rather high crystallinity.

Raman spectrum of (Mg, Fe) SiO₃-glass displays only two broad bands at 978 and 665 cm⁻¹ (Figure 4(c)), and these two bands could be attributed to Si-O stretching vibrations of SiO₄ tetrahedra and to the inter-tetrahedral Si-O-Si vibration, respectively (McMillan, 1984a, 1984b).
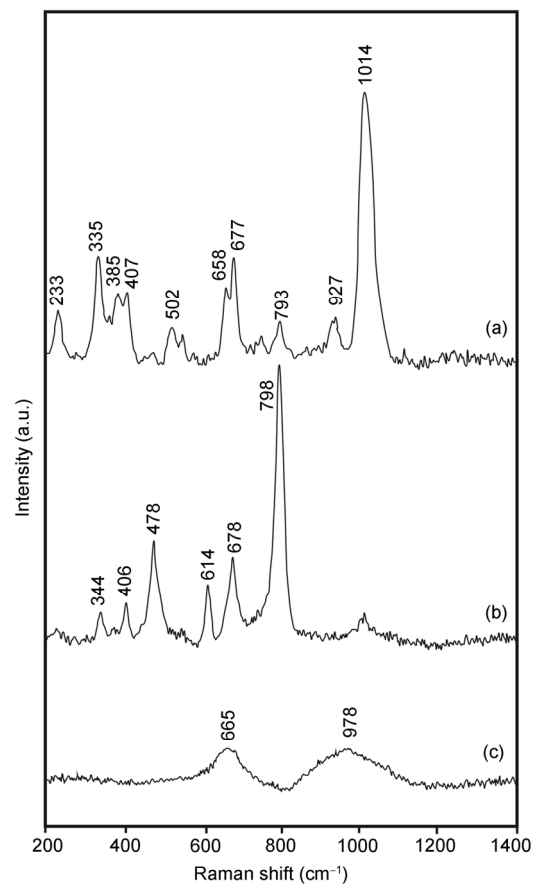

Figure 4　Raman spectra of low-Ca pyroxene (a), akimotoite (b), and amorphized perovskite (c) in the Suizhou meteorite.

3 Discussion

Static high-pressure experiments demonstrated that low-Ca pyroxene could transform to akimotoite at 17.5–27.5 GPa and 600–2050°C (Liu, 1976; Presnell, 1995). The transformation of enstatite to akimotoite requires temperatures in excess of 1550°C at 22 GPa (Hogrefe et al., 1994). Two scenarios or models were proposed for the formation mechanisms of akimotoite in shock-metamorphosed meteorites: (1) Solid state transformation from low-Ca pyroxene or clinopyroxene to akimotoite under high pressures and temperatures (Tomioka and Fujino, 1997, 1999); (2) crystallization from a chondritic silicate melt under high pressures and temperature (Sharp et al., 1997). The first model is mainly based on a topotaxial relationship between akimotoite with neighboring pyroxene, and the same composition between pyroxene and akimotoite (Tomioka and Fujino, 1997, 1999), and the second one is because akimotoite is enriched in CaO, Al_2O_3 and Na_2O, and occurs as small prismatic or plate-like idiomorphic crystals in the shock vein matrix (Sharp et al., 1997).

Akimotoite in the Suizhou shock veins has an identical composition as its low-Ca pyroxene (Table 1). It shows the akimotoite was crystallized from an isochemical material transformed from previous low-Ca pyroxene. Irregular distribution of akimotoite layers of up to 4 μm in width within pyroxene (Figure 2) shows that there are no crystallographic relationship between akimotoite and its parental pyroxene. Such occurrence can only be explained by nucleation and growth along fractures and cracks in pyroxene. Jagged teethes on the boundaries of akimotoite layers are indicative of growth of crystals. Similar phenomena are very common in shock-metamorphosed chondritic meteorites. One typical example is that the lamellar ringwoodite had incoherently nucleated and grown along planar and irregular fractures in olivine in chondritic area of meteorites (Chen et al., 2006, 2007), which are attributed to strong crystal distortion of olivine in the regions of fractures and cracks during shock-induced deformation (Chen et al., 2006). Abundant defects in deformed crystals are available for phase transformation because it will significantly modify and enhance the solid-state reactivity and the kinetics of nucleation of high-pressure phase (Thadhani, 1994). There is no question that abundant defects would be produced on the two sides near fracture and crack in minerals and also at grain boundaries because the concentration of stress and the elevation of temperature during shock. As a result, akimotoite preferentially nucleates and crystallizes along fractures and cracks in pyroxene.

In the pyroxene close to the shock veins, the formation of zonal akimotoite in between pyroxene and $MgSiO_3$-glass is also related to the abundant crystal defects as well as higher pressures and temperatures (Figure 3). The shock veins were formed mainly because of shearing, compression, and friction melting within the meteorite (Stöffler et al., 1991).

The pyroxene in contact with shock veins was strongly deformed and contains abundant defects, which is available for the transformation of pyroxene to akimotoite.

Static high-pressure experiments indicated that $MgSiO_3$-perovskite crystallizes above 23 GPa and at ~ 2000°C (Liu, 1976; Gasparik, 1993), and that low-Ca pyroxene could transform to akimotoite at 17.5–27.5 GPa and 600–2050°C (Liu, 1976; Presnell, 1995) or that the transformation of enstatite to akimotoite requires temperatures in excess of 1550°C at 22 GPa (Hogrefe et al., 1994). The pressure and temperature history in the shock veins of meteorites can be well-constrained by high-pressure mineral assemblage (Chen et al. 1996). Based on the high-pressure melting experimental data on a chondritic meteorite by Agee et al. (1995), the assemblage of majorite-pyrope garnet, magnesiowüstite, and ringwoodite in the shock veins of the Suizhou meteorite should have crystallized at pressures up to 23 GPa and temperatures to 2000°C (Chen et al. 2004; Xie et al. 2001). The occurrence of zonal $MgSiO_3$-glass is in contact with the shock veins (Figure 3), which could indicate the pressures and temperatures in the area of zonal $MgSiO_3$-glass was similar or close to those of the shock veins in the Suizhou meteorite. The pressure and temperature regime of 23 GPa and 2000°C within the shock veins should have been available for the transformation of pyroxene to $MgSiO_3$-perovskite. Previous investigation suggests that the $MgSiO_3$-glass occurring in the shock veins of Suizhou meteorite is vitrified perovskite formed after pressure release at post-shock temperature (Chen et al., 2004). According to heating experiments of Durben et al. (1992), the crystalline $MgSiO_3$-perovskite trends to decompose to amorphous phase near the ambient pressure at moderate temperatures. Amorphized perovskite interwoven with akimotoite grains was also observed in the shock veins of the Tenham chondrite (Ferroir et al., 2008). Therefore, we suggest the region of pyroxene in contact with shock veins was transformed to perovskite during shock compression and then became amorphized after pressure release.

In the Suizhou meteorite, the occurrence of both the akimotoite-layers and the zonal akimotoite occur in parental pyroxene show a shock-induced solid-state transformation of pyroxene to akimotoite. According to the very close ocurrence to the shock vein wall and the results of above mentioned experiments (Liu, 1976; Presnell, 1995; Hogrefe et al., 1994), we estimate that akimotoite in the Suizhou meteorite might be formed at about 22~23 GPa and 1550°C. This indicates that akomotoite can be formed at similar pressure but at much lower temperature than perovskite (23 GPa, 2000°C). In addition, the high-pressure and high-temperature phase diagram of $MgSiO_3$ reported by Presnell (1995), under a given pressure, ilmenite (akimotoite) and perovskite phases can be formed at wide range of temperature, from about 600°C to 2030°C, respectively. Hence, we assume that the spatial relationship among pyroxene, akimotoite and $MgSiO_3$-glass (possibly vitrified perovskite)

in the Suizhou meteorite can be well explained by a temperature gradient from the vein wall to the unmelted chondritic meteorite.

Agee C B, Li J, Shannon M C, et al. 1995. Pressure-temperature phase diagram for Allende meteorite. J Geophys Res, 100: 17725–17740

Chen M, Sharp T G, El Goresy A, et al. 1996. The majorite-pyrope+ magnesiowustite assemblage: Constrains on the history of shock veins in chondrites. Science, 271: 1570–1573

Chen M, Shu J F, Xie X D, et al. 2003a. Natural CaTi$_2$O$_4$-structured FeCr$_2$O$_4$ polymorph in the Suizhou meteorite and its significance in mantle mineralogy. Geochim Cosmochim Acta, 67: 3937–3942

Chen M, Shu J F, Mao H K, et al. 2003b. Natural occurrence and synthesis of two new postspinel polymorphs of chromite. Proc Nat Acad Sci USA, 100: 14651–14654

Chen M, Xie X D, El Goresy A. 2004. A shock-produced (Mg, Fe) SiO$_3$ glass in the Suizhou meteorite. Meteorol Planet Sci, 39: 1797–1808

Chen M, Li H, El Goresy A, et al. 2006. Fracture-related intracrystalline transformation of olivine to ringwoodite in the shocked Sixiangkou meteorite. Meteorit Planet Sci, 41: 731–737

Chen M, Chen J, Xie X et al. 2007. A microstructural investigation of natural lamellar ringwoodite in olivine of the shocked Sixiangkou chondrite. Earth Planet Sci Lett, 264: 277–283

Chen M, Shu J F, Mao H K. 2008. Xieite, a new mineral of high-pressure FeCr$_2$O$_4$ polymorph. Chin Sci Bull, 53: 3341–3345

Durben D J, Wolf G, 1992. High-temperature behavior of metastable MgSiO$_3$ perovskite: A Raman spectroscopic study. Am Mineral, 77: 890–893

Ferroir T, Beck P, Van de Moortèle B, et al. 2008. Akimotoite in the Tenham meteorite: Crystal chemistry and high-pressure transformation mechanisms. Earth Planet Sci Lett, 275: 26–31

Gasparik P. 1993. The role of volatiles in the transition zone. J Geophys Res, 98: 4287–4299

Hogrefe A, Rubie D C, Sharp T G, et al. 1994. Metastability of enstatite in deep subducting lithosphere. Nature, 372: 351–353

Liu L G. 1976. The high-pressure phases of MgSiO$_3$. Earth Planet Sci Lett, 31: 200–208

McMillan P. 1984a. Structure studies of silicate glasses and melts— Applications and limitations of Raman spectroscopy. Am Mineral, 69: 622–644

McMillan P. 1984b. A Raman spectroscopic study of glasses in the system CaO-MgO-SiO$_2$. Am Mineral, 69: 649–659

Nagy Sz, Bérczi Sz, Józsa S, et al. 2010. Olivine and pyroxene high- pressure polymorphs in melt veins of the strongly shocked NWA 5011 meteorite sample. In: 41st Lunar Planetary Science Conference, Houston, No.1228

Ohtani E, Kimura Y, Kimura M, et al. 2004. Formation of high-pressure minerals in shocked L6 chondrite Yamato 791384: Constraints on shock conditions and parent body size. Earth Planet Sci Lett, 227: 505–515

Presnell D C. 1995. Phase diagrams of earth-forming minerals. In: Ahrens T J, ed. Mineral Physics and Crystallography: A Handbook of Physical Constants. Amer Geophys Union. 248–268

Thadhani N N. 1994. Shock induced and shock-assisted solid-state chemical reactions in powder mixtures. J Appl Phys, 76: 2129–2138

Tomioka N, Fujino K. 1997. Natural (Mg, Fe) SiO$_3$-ilmenite and – perovskite in the Tenham meteorite. Science, 277: 1084–1086

Tomioka N, Fujino K. 1999. Akimotoite, (Mg, Fe) SiO$_3$, a new silicate mineral of the ilmenite group in the Tenham chondrite. Am Mineral, 84: 267–271

Sharp T G, Lingemann C M, Dupas C, et al. 1997. Natural occurrence of MgSiO$_3$-ilmenite and evidence for MgSiO$_3$-perovskite in a shocked L chondrite. Science, 277: 352–255

Stöffler D, Keil K, Scott E R D. 1991. Shock metamorphism of ordinary chondrites. Geochim Cosmochim Acta, 55: 3845–3867

Xie X D, Chen M, Wang D Q. 2001. Shock-related mineralogical features and *P-T* history of the Suizhou L6 chondrite. Eur J Mineral, 13: 1177–1190

Xie X D, Minitti M E, Chen M, et al. 2003. Tuite, γ-Ca$_3$(PO$_4$)$_2$, a new phosphate mineral from the Suizhou L6 chondrite. Eur J Mineral, 15: 1001–1005

Xie X D, Chen M, Wang D Q. 2005. Two types of silicate melts in naturally shocked meteorites. In: Papers and abstracts of the 5th Annual Meeting of IPACES, Guangzhou. 12–14

Xie X D, Sun Z Y, Chen M. 2011. The distinct morphological and petrological features of shock melt veins in the Suizhou L6 chondrite. Meteorit Planet Sci, 46: 459–469

Xie Z D, Sharp T G. 2004. High-pressure phases in shock-induced melt veins of the Umbarger L6 chondrite: Constraints of pressure. Meteor Planet Sci, 39: 2043–2054

Zhang A C. 2006. Pyroxene polymorphs in melt veins of the heavily shocked Sixiangkou L6 chondrite. Eur J Mineral, 18: 719–726